

Microscopic Origin of Structural Disorder in $\delta - \text{NbN}$: Correlation of Superconductivity and Electronic Structure

Shailesh Kalal,¹ Sanjay Nayak,² Akhil Tayal,³ Jens Birch,² Rajeev Rawat,¹ and Mukul Gupta^{1,*}

¹*UGC-DAE Consortium for Scientific Research,
University Campus, Khandwa Road, Indore-452 001, India*

²*Thin Film Physics Division, Department of Physics,
Chemistry and Biology (IFM), Linköping University, SE-581 83, Linköping, Sweden*

³*Deutsches Elektronen-Synchrotron DESY, Notkestrasse 85, D-22607 Hamburg, Germany*

(Dated: October 12, 2020)

Rock-salt type niobium nitride ($\delta - \text{NbN}$) is a well-known superconductor having superconducting transition temperature (T_C) ≈ 18 K and a large superconducting gap ≈ 3 meV. The T_C of $\delta - \text{NbN}$ thin film exhibits a large scattering irrespective of the growth conditions and lattice parameter. In this work, we investigate the atomic origin of suppression of T_C in $\delta - \text{NbN}$ thin film by employing combined methods of experiments and ab-initio simulations. Sputtered $\delta - \text{NbN}$ thin films with different disorder were analyzed through electrical resistivity and x-ray absorption spectroscopy. A strong correlation between the superconductivity and the atomic distortion induced electronic reconstruction was observed. The theoretical analysis revealed that under N-rich growth conditions, atomic and molecular N-interstitial defects assisted by cation vacancies form spontaneously and are responsible for the suppression of T_C in $\delta - \text{NbN}$ by smearing its electronic densities of states around Fermi level.

Superconducting niobium nitride (NbN) thin films have been extensively used to fabricate modern technological devices like: single photon detector [1], hot electron bolometer [2], Josephson junction [3], high field superconducting magnet [4], nano-electromechanical systems and high-pressure devices [5] etc. The choice of NbN for several technological applications has been motivated due to its relatively higher superconducting transition temperature ($T_C \approx 18$ K) and high superconducting energy gap ($\Delta(0) \approx 3$ meV) among transition metal nitrides (TMNs) [6, 7]. The superior mechanical stability and ease of fabrication of NbN with cost-effective technique such as sputtering is another reason for its popular choice to fabricate devices [8]. Among its several polymorphs, $\delta - \text{NbN}$ (space group: $Fm\bar{3}m$) shows the highest value of T_C owing to its stronger electron-phonon coupling caused by larger electronic densities of states around Fermi energy (E_F) and lower Debye temperature (Θ_D) [9, 10].

One of the crucial issues in the development of superconducting NbN based technology is to achieve the optimum T_C . In the literature, it is well documented that the growth techniques and conditions play a vital role in determining T_C . Polakovic et al. [11] have reported that, T_C as a function of N_2 gas pressure shows a dome like behavior with maximum value of ≈ 14 K at a specific range of N_2 concentration (17-20%). Similar results have been reported by Choudhuri et al. [12] where T_C of NbN thin films maximizes at certain nitrogen partial pressure. Through Hall measurements Chockalingam et al. [13] demonstrated that T_C of NbN thin films deposited at different R_{N_2} was governed by carrier density caused by Nb and/or N vacancies concentration. However, this work does not

shed light on a drastic reduction of the carrier density with samples grown at higher N_2 partial pressure (R_{N_2}). Similar results have been widely reported in the literature [14–16]. Often, the atomic disorder has been attributed to the reduction of the T_C in this superconductor [16–18].

Thus, to uncover the microscopic origin of the widely speculated structural disorder and consequently its effect on superconductivity, we synthesize $\delta - \text{NbN}$ thin films using a dc-magnetron sputtering (details of the deposition parameters are discussed in section I of supplementary material (SM) [19]). Disorder in the films is tuned by varying the R_{N_2} during the deposition process. Samples have been thoroughly characterized using complementary characterization tools. A combined approach of experiments and first-principles simulations is adopted to reach the conclusion.

Table I. Measured lattice parameter (LP) and superconducting transition temperature (T_C) of $\delta - \text{NbN}$ samples. The T_C could not be observed within the instrumental limit for the sample grown at nitrogen partial pressure (R_{N_2}) = 30, 65, 100%.

R_{N_2} (%)	LP (± 0.006 Å)	T_C (K)
16	4.376	12.8
25	4.415	6.9
30	4.421	-
65	4.486	-
100	4.505	-
Theoretical (this work)	4.41	-
Experimental [6]	4.40	17.3
Theoretical [20]	4.45	18.2

A detailed report on structural and transport characterization of grown films has been published elsewhere [21] where XRD result confirms that the sam-

* mgupta@csr.res.in

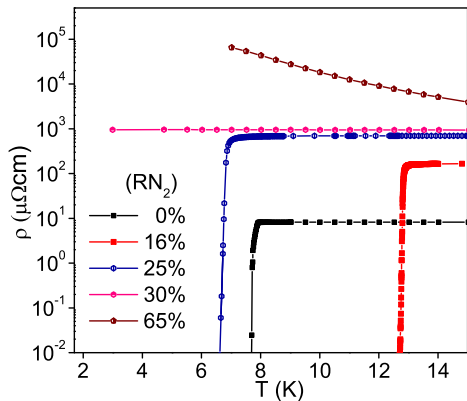


Figure 1. Temperature dependent electrical resistivity (ρ) of samples deposited at $R_{N_2} = 0, 16, 25, 30, 65\%$. Here, $R_{N_2} = 100\%$ sample not included as its $\rho > 10^5$.

ple grown at $R_{N_2} = 0\%$ is a pure Nb with bcc structure and the sample grown at $R_{N_2} = 16, 25, 30, 65, 100\%$ have a single phase of NbN with rock-salt type crystal structure ($\delta - \text{NbN}$). The T_C (defined as the point where ρ falls down to 10% of its normal value) of the grown films are obtained from standard four probe temperature dependent electrical resistivity (ρ) measurements are presented in Fig. 1. The values of R_{N_2} , LP and T_C are given in table I where a strong correlation between structure and superconductivity is noticed. Here with increase in R_{N_2} , the LP is continuously increasing and consequently a reduction in the T_C is seen.

In order to understand the effect of growth conditions on the electronic structure, we performed element specific x-ray absorption near edge spectroscopy (XANES) measurements both at Nb and N K-edges as shown in Fig. 2 (a) and (b), respectively. We note that Nb K-edge splits into two components $K1$ and $K2$ (see inset of Fig. 2 (a)). The initial rise $K1$ is due to the transitions from $1s$ core level to unoccupied admixed $4d-5p$ levels while the second absorption rise $K2$ arises due to transitions from the $1s$ core level to the Laporte-allowed states of pure $5p$ symmetry [22, 23]. The absorption edge of sample deposit at $R_{N_2} = 16\%$ is shifted to higher energy by 3 eV as compared to elemental Nb (see inset of Fig. 2 (a)), which indicates that Nb atom bears positive charge due to the formation of NbN compound. Further, with $R_{N_2} \geq 25\%$ d band is delocalizing around the Fermi level (E_{K1}).

Similarly, we observed clear changes in the line shape of N K-edge spectra with increase in R_{N_2} (see Fig. 2 (b)). A sharp transition at threshold of around 400 eV arises for the sample deposit at $R_{N_2} = 16\%$. Here, we note presence of electronic sub-band transition levels labeled as a, b, c, d . DOS analysis reveals (see Fig. S2 of SM) these features are results of transition from N- $1s$ core level to unoccupied N- $2p$ orbitals. It is well-known that the TMNs in octahedral bonding coordination (e.g. $\delta - \text{NbN}$) metal d orbitals splits into two electronic sub-bands (e_g and t_{2g}) owing to its hybridized characteristics of N- $2p$ orbitals [24]. Feature a (centred at 402.8 eV) in N K-

edge XANES spectra is a consequence of hybridized N- $2p$ and t_{2g} level of Nb- $4d$ orbitals, feature b (centred at 406.8 eV) is a consequence of hybridized N- $2p$ and e_g level of Nb- $4d$ orbitals. The feature c and d arises due to higher order hybridization between N- $2p$ and Nb- $5s-5p$ orbitals. Further at $R_{N_2} = 25\%$, feature b become broad and at $R_{N_2} = 30\%$, sharp a^* feature (404.9 eV) arises in between a and b , whose intensity is gradually increases with increase in R_{N_2} .

To identify the atomic origin of above mentioned features, we simulate N K-edge XANES spectra for multiple defect configurations using multi scattering theory (see Fig. S1 of SM [19]). We obtained the relaxed atomic structure of various point defects: (i) isolated N-vacancy (V_N), (ii) multiple N-vacancy ($2V_N$), (iii) Nb vacancy (V_{Nb}), (iv) N interstitial (N_i), (v) N antisite (N_{Nb}), (vi) Schottky type defect ($V_N - V_{Nb}$), and (vii) interstitial N_2 molecules (N_{2i}) from SIESTA codes and used them to construct atomic cluster for simulation of ab-initio XANES spectra (computational details of simulations are given in section II of SM [19]). First, to establish the credibility of numerical parameters used in simulations, we obtained N K-edge spectra for pristine $\delta - \text{NbN}$. Clearly, features a, b, c , and d are reproduced in simulations. The experimental spectrum obtained for the sample grown at $R_{N_2} = 16\%$ is in well agreement with the theoretically calculated spectra of $\delta - \text{NbN}$ having V_{Nb} (see Fig. 2 (b) and (c)). A thorough comparison between experimental (Fig. 2 (b)) and simulated (Fig. 2 (c)) XANES spectra of N K-edge, revealed that appearance of a^* peak centred around 404.9 eV for the sample grown at higher R_{N_2} is probably a signature of either N_i or N_{2i} defects in $\delta - \text{NbN}$.

Gall et al. [25] studied the energetic of defect formation in TMNs and suggested a cation vacancy (V_{Nb}) is the most stable defect in $\delta - \text{NbN}$, consistent with our estimation of formation energy (FE). FE plot for various defect configurations is shown in Fig. 3. Estimated FE of V_{Nb} under N-rich growth condition is -0.74 eV. Work of Gall et al. [25] predicted that FE of N_i is very high, which is again consistent with our estimation of high FE = 1.55 eV at N-rich conditions. Further we find even under N-rich conditions, FE of molecular nitrogen (N_{2i}) in $\delta - \text{NbN}$ is very high (4.51 eV). High FE of N_i and N_{2i} in $\delta - \text{NbN}$ clearly suggests that they will not form spontaneously and their concentration in $\delta - \text{NbN}$ should be negligible. Interestingly, we find that when V_{Nb} and N_i are in a complex form ($V_{Nb}-N_i$) their FE reduces and under N-rich condition, we estimate it to be -0.43 eV (see Fig. 3). Also the estimated binding energy (BE) of $V_{Nb}-N_i$ is too high (1.26 eV). The positive BE indicates the preferential stability of the defect complex and higher the magnitude means better the stability (details of method to estimate BE is discussed in section II to SM [19]). Similarly when N_{2i} incorporated near V_{Nb} site, it forms $V_{Nb}-N_{2i}$ defect complex and its FE is 2.21 eV (see Fig.3). The estimated BE of the $V_{Nb}-N_{2i}$ is 1.56 eV. The FE of N_{2i} further reduces to 0.02 eV when it get coupled with two nearest neighbour V_{Nb} sites (see Fig.3) with

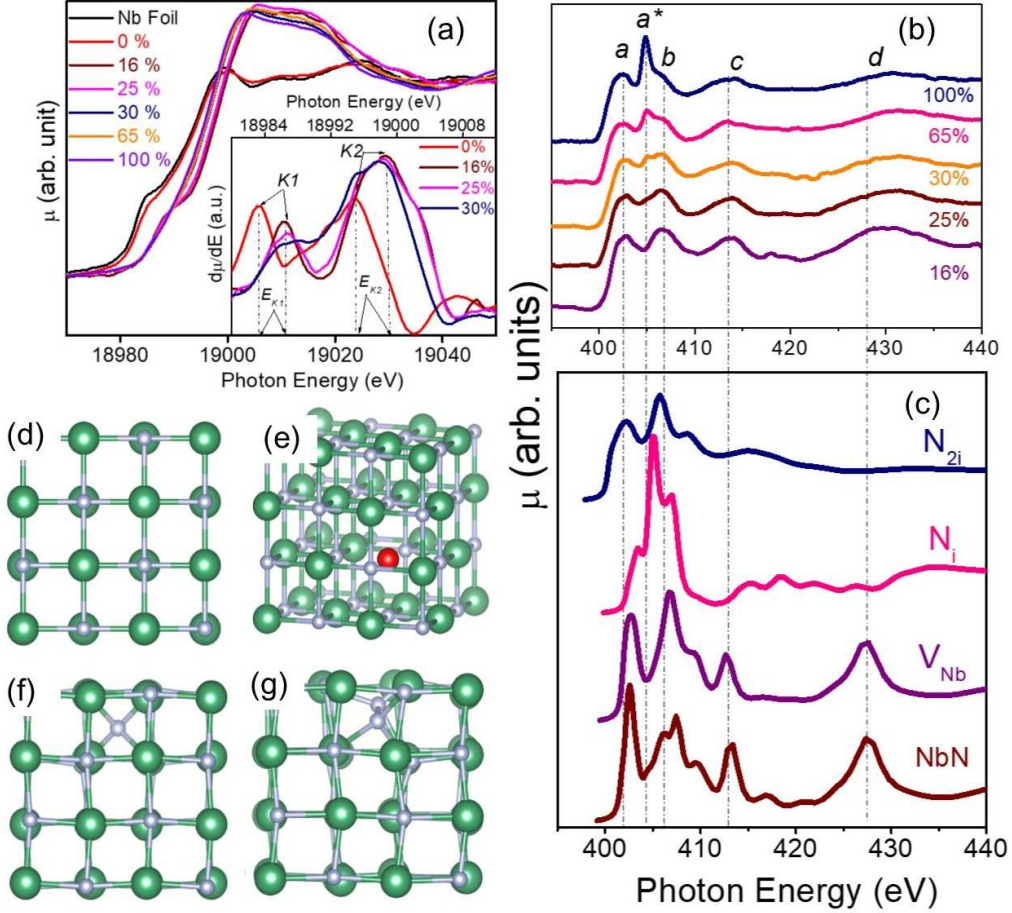


Figure 2. (a) Nb K-edge XANES spectra with inset showing first derivative. (b) N K-edge XANES spectra and (c) simulated N K-edge XANES spectra for various defect configurations. Ball-and-stick models of different δ -NbN configurations used in DFT and multiple scattering theory calculations are presented: (d) pristine δ -NbN, (e) with Nb vacancy (V_{Nb}), (f) with interstitial nitrogen (N_i) and (g) with molecular nitrogen (N_{2i}).

a very high BE of 5.96 eV. These observations clearly establish that the interstitial atomic (N) and molecular nitrogen (N_2) can be stabilized in δ -NbN through cation (Nb) vacancies.

Further, we analyze the effect of these defects to the atomic structure of δ -NbN. The obtained relaxed LP of δ -NbN is noted to be 4.41 Å. We find that 3.125% of V_{Nb} in δ -NbN reduces the unit cell volume by 0.06%. While $V_{\text{Nb}}-N_i$ increases the unit cell volume by 0.025% and defect complex $V_{\text{Nb}}-N_{2i}$ causes shrinking of unit cell volume by 0.020%. A comparison between experimentally obtained LP (and hence volume, see table I) and theoretically computed volumes suggests that $V_{\text{Nb}}-N_i$ is predominant in the samples grown with $R_{N_2} > 16\%$ and their concentration increases with increase in R_{N_2} . The smaller LP (see table I) of δ -NbN thin film grown at $R_{N_2} = 16\%$ suggest a presence of higher concentration of V_{Nb} in it. Also the estimated lattice relaxation energy, $\Delta E_c [= E_{\text{tot}}$ (without ionic relaxation) - E_{tot} (with ionic relaxation)] of δ -NbN with point defects V_{Nb} , V_N , N_i , $V_{\text{Nb}}-N_i$, N_{2i} , $V_{\text{Nb}}-N_{2i}$, and $2V_{\text{Nb}}-N_{2i}$ is 15, 10, 102, 107, 163, 160, and 172 meV/atom, respectively.

Higher values of ΔE_c for interstitial defects suggest a substantial lattice distortion of δ -NbN, in agreement with the increment of disorder in the δ -NbN films with increase in R_{N_2} .

Next, we shall discuss the role of these point defects (if any) on the superconducting properties of δ -NbN thin films. Using the value of electron-phonon coupling constant (λ), T_c for the strong coupling superconductors can be obtained via McMillan-Allen-Dynes formalism [9, 13, 26, 27], given by:

$$T_c = \frac{\omega_{\log}}{1.2} \exp \left[\frac{-1.04(1 + \lambda)}{\lambda - \mu^*(1 + 0.62\lambda)} \right] \quad (1)$$

where ω_{\log} is a logarithmic average of phonon frequency, μ^* is the averaged screened electron-electron interaction. The λ further calculated as $\lambda = [N(\epsilon_F)/\langle\omega^2\rangle] \sum_i \langle I^2 \rangle_i / M_i$, where M_i is the atomic mass of i^{th} atom and $\langle I^2 \rangle_i$ is the square of the electron-phonon coupling matrix element averaged over the Fermi surface [26, 27]. $N(\epsilon_F)$ is the electronic density of states at the Fermi level. The $\langle\omega^2\rangle$ can be further approximated as $0.5\Theta_D^2$, where Θ_D is the Debye temperature [28]. From eq. 1, it is quite evident that

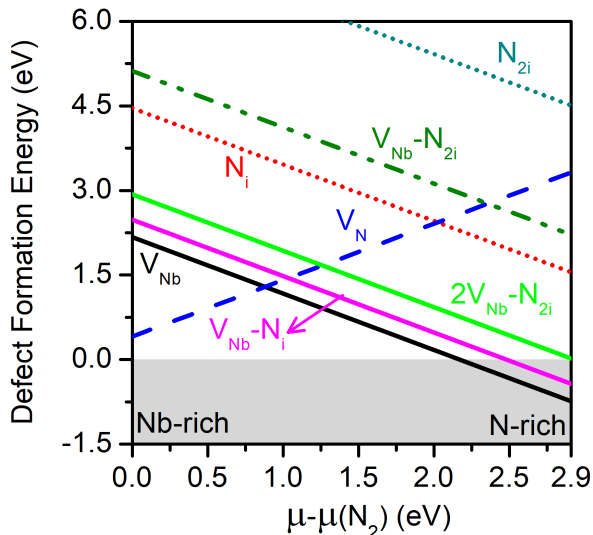


Figure 3. Formation energy as a function of chemical potential of N_2 for Nb vacancy (V_{Nb}), nitrogen vacancy (V_N), interstitial nitrogen (N_i), molecular nitrogen (N_{2i}), combination of niobium vacancy with interstitial nitrogen ($V_{Nb}-N_i$), combination of niobium vacancy with molecular nitrogen ($V_{Nb}-N_{2i}$), and combination of multiple niobium vacancy with interstitial nitrogen ($2V_{Nb}-N_{2i}$) defect configurations.

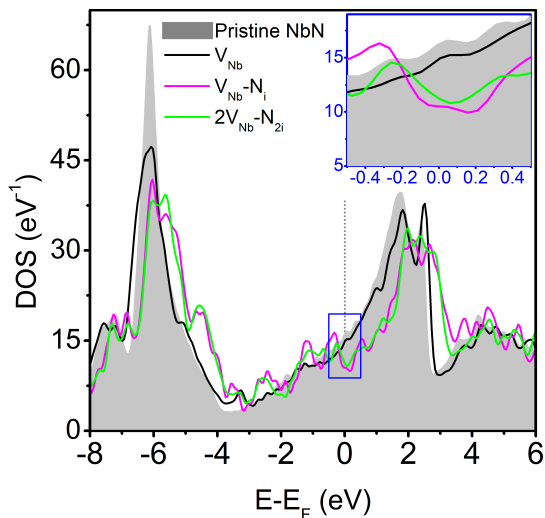


Figure 4. Calculated total density of state (DOS) for stoichiometric δ -NbN along with Nb vacancy (V_{Nb}), combination of Nb vacancy (V_{Nb}) with interstitial nitrogen (N_i), and combination of multiple Nb vacancy with molecular nitrogen ($2V_{Nb}-N_{2i}$) configurations. Inset shows expanded view of Fermi level. Here, Fermi level is set to 0 eV.

T_C is sensitive to the $N(\epsilon_F)$. Thus, we computed the electronic DOS of NbN with previously determined dominant defects and presented in Fig. 4. A strong smearing in the electronic structure is visible due to the formation of $V_{Nb}-N_i$ or $2V_{Nb}-N_{2i}$ defects complex in δ -NbN (see Fig. 4). DOS calculations shows that $N(\epsilon_F)$ of pristine δ -NbN ($2 \times 2 \times 2$ supercell) is 16.26 states.eV $^{-1}$. For 3.125% of V_{Nb} , $N(\epsilon_F)$ reduces

to 14.75 states.eV $^{-1}$. The computed $N(\epsilon_F)$ for $V_{Nb}-N_i$ and $2V_{Nb}-N_{2i}$ are 10.50 and 11.15 states.eV $^{-1}$, respectively. We estimate T_C by substituting the values of ω_{log} (=269 K), Θ_D (=637 K), μ^* (=0.10) computed for δ -NbN in Ref. 9 and the normalized electronic DOS from our simulations in eq. 1. For pristine δ -NbN Gou et al. computed T_C = 18.26 K, a little higher than experimentally obtained ones [9]. Using the SIESTA, computed $N(\epsilon_F)$ of δ -NbN with 3.125% V_{Nb} in eq.1, estimate of T_C to be 15.78 K. The experimental T_C of δ -NbN sample grown at R_{N_2} =16% is 12.8 K, hinting concentration of V_{Nb} is higher than 3.125% in it. Further using the $N(\epsilon_F)$ of $V_{Nb}-N_i$ and $2V_{Nb}-N_{2i}$ configurations in eq. 1 results into T_C of 7.18 K and 8.44 K, respectively. These values are in excellent agreement with the experimentally obtained T_C = 6.9 K of sample grown at R_{N_2} =25%. The absence of superconducting transition (down to 3 K) in the samples grown at $R_{N_2} \geq 30\%$ is possibly due to the presence of a large disorder in the films, which occurs in δ -NbN films due to the presence of a large concentration of N-interstitial related defects. We estimate a 50% reduction in $N(\epsilon_F)$ as compared to the pristine δ -NbN can push the T_C to below 3 K.

Thus, here we unveil the atomic structure of disordered δ -NbN responsible for suppression of superconducting transition temperature. Under N-rich growth conditions, spontaneously formed cation vacancies are responsible for the stabilization of N-interstitial defects in δ -NbN thin films which are otherwise unfavourable with high formation energies. The positive binding energy of the cation vacancies and anion interstitial defect complex further cements their bonding in the crystal. Formation of the N-interstitial defect complex in δ -NbN causes strong smearing of electronic structure by creating atomic disorder in the films and thus a significant reduction in the $N(\epsilon_F)$ which strongly influencing the electron-phonon coupling strength and consequently reduces the T_C . Increase in the T_C of vacuum annealed δ -NbN [29–31] and degradation of superconducting properties at N_2 atmosphere [32, 33] further support our proposed mechanism. Based on above analysis we suggest that to obtain δ -NbN with high T_C , films should be grown at Nb-rich conditions to avoid N interstitial defects and annealing of samples in a vacuum is recommended to eliminate residual N atoms.

In summary, we have uncovered the microscopic origin of growth parameter dependence on the T_C of δ -NbN. By probing the electronic structure of disordered δ -NbN samples, we identify point defect complexes consisting of cation vacancies with atomic anion interstitial [$V_{Nb}-N_i$] and cation vacancies with interstitial molecular nitrogen [$nV_{Nb}-N_{2i}$] are responsible for suppression of the T_C in NbN films grown at higher nitrogen partial pressure (R_{N_2}). The suppression of the T_C is caused by smearing of electronic structure and reduction of electronic DOS around Fermi energy due to the formation of point defect complex. We show that stabilization of atomic and molecular nitrogen in δ -NbN is assisted by cation vacancies. Es-

timated T_C of $\delta - \text{NbN}$ with dominant defects identified from first-principles simulations are in good agreement with the experimentally obtained values.

ful to A. K. Sinha, Alok Banerjee, and D. M. phase for support and encouragement. This work is supported through India-DESY project.

ACKNOWLEDGMENTS

We thank L. Behera, R. Sah and A. Wadikar for technical help provided in experiments. We are thank-

-
- [1] G. Goltsman, O. Okunev, G. Chulkova, A. Lipatov, A. Semenov, K. Smirnov, B. Voronov, A. Dzardanov, C. Williams, and R. Sobolewski, *Applied physics letters* **79**, 705 (2001).
 - [2] J. J. Baselmans, M. Hajenius, J. Gao, T. Klapwijk, P. De Korte, B. Voronov, and G. Goltsman, *Applied physics letters* **84**, 1958 (2004).
 - [3] Y. Yu, S. Han, X. Chu, S.-I. Chu, and Z. Wang, *Science* **296**, 889 (2002).
 - [4] R. Kampwirth, D. Capone, K. Gray, and A. Vicens, *IEEE Transactions on Magnetics* **21**, 459 (1985).
 - [5] X. Blase, E. Bustarret, C. Chapelier, T. Klein, and C. Marcenat, *Nature materials* **8**, 375 (2009).
 - [6] K. Keskar, T. Yamashita, and Y. Onodera, *Japanese Journal of Applied Physics* **10**, 370 (1971).
 - [7] A. Kamlapure, M. Mondal, M. Chand, A. Mishra, J. Jesudasan, V. Bagwe, L. Benfatto, V. Tripathi, and P. Raychaudhuri, *Applied Physics Letters* **96**, 072509 (2010).
 - [8] A. Kamlapure, M. Mondal, M. Chand, A. Mishra, J. Jesudasan, V. Bagwe, L. Benfatto, V. Tripathi, and P. Raychaudhuri, *Applied Physics Letters* **96**, 072509 (2010).
 - [9] K. R. Babu and G.-Y. Guo, *Physical Review B* **99**, 104508 (2019).
 - [10] Y. Zou, X. Qi, C. Zhang, S. Ma, W. Zhang, Y. Li, T. Chen, X. Wang, Z. Chen, D. Welch, *et al.*, *Scientific reports* **6**, 22330 (2016).
 - [11] T. Polakovic, S. Lendinez, J. E. Pearson, A. Hoffmann, V. Yefremenko, C. L. Chang, W. Armstrong, K. Hafidi, G. Karapetrov, and V. Novosad, *APL Materials* **6**, 076107 (2018).
 - [12] S. Chaudhuri, M. Nevala, T. Hakkarainen, T. Niemi, and I. Maasilta, *IEEE transactions on applied superconductivity* **21**, 143 (2010).
 - [13] S. Chockalingam, M. Chand, J. Jesudasan, V. Tripathi, and P. Raychaudhuri, *Physical Review B* **77**, 214503 (2008).
 - [14] A. E. Dane, A. N. McCaughan, D. Zhu, Q. Zhao, C.-S. Kim, N. Calandri, A. Agarwal, F. Bellei, and K. K. Berggren, *Applied Physics Letters* **111**, 122601 (2017).
 - [15] T. Shiino, S. Shiba, N. Sakai, T. Yamakura, L. Jiang, Y. Uzawa, H. Maezawa, and S. Yamamoto, *Superconductor Science and Technology* **23**, 045004 (2010).
 - [16] M. Chand, A. Mishra, Y. Xiong, A. Kamlapure, S. Chockalingam, J. Jesudasan, V. Bagwe, M. Mondal, P. Adams, V. Tripathi, *et al.*, *Physical Review B* **80**, 134514 (2009).
 - [17] S. Chockalingam, M. Chand, J. Jesudasan, V. Tripathi, and P. Raychaudhuri, in *Journal of Physics: Conference Series*, Vol. 150 (IOP Publishing, 2009) p. 052035.
 - [18] C. Carbillet, V. Cherkez, M. Skvortsov, M. Feigel'man, F. Debontridder, L. Ioffe, V. Stolyarov, K. Ilin, M. Siegel, C. Noûs, *et al.*, *Physical Review B* **102**, 024504 (2020).
 - [19] "Supplemental material for- Microscopic Origin of Structural Disorder in $\delta - \text{NbN}$: Correlation between Superconductivity and Electronic Structure, providing experimental, computational details".
 - [20] K. R. Babu and G.-Y. Guo, *Physical Review B* **99**, 104508 (2019).
 - [21] S. Kalal, M. Gupta, and R. Rawat, *Journal of Alloys and Compounds* , 155925 (2020).
 - [22] J. Muller, O. Jepsen, O. K. Andersen, and J. Wilkins, *Physical Review Letters* **40**, 720 (1978).
 - [23] W. Agnieszka and K. Barbara, *Journal of Non-Crystalline Solids* **358**, 969 (2012).
 - [24] J. G. Chen, *Surface Science Reports* **30**, 1 (1997).
 - [25] K. Balasubramanian, S. V. Khare, and D. Gall, *Acta Materialia* **159**, 77 (2018).
 - [26] P. Allen and R. Dynes, *Journal of Physics C: Solid State Physics* **8**, L158 (1975).
 - [27] W. L. McMillan, *Physical Review* **167**, 331 (1968).
 - [28] L. Liu, X. Wu, R. Wang, X. Nie, Y. He, and X. Zou, *Crystals* **7**, 111 (2017).
 - [29] E. J. Cukauskas, S. Qadri, and W. L. Carter, *Journal of applied physics* **65**, 2053 (1989).
 - [30] W. Carter and E. Cukauskas, *IEEE Transactions on Magnetics* **23**, 847 (1987).
 - [31] T. Farrahi, M. E. Cyberey, M. B. Eller, and A. W. Lichtenberger, *IEEE Transactions on Applied Superconductivity* **29**, 1 (2019).
 - [32] M. Hatano, T. Nishino, and U. Kawabe, *Journal of Vacuum Science & Technology A: Vacuum, Surfaces, and Films* **6**, 2381 (1988).
 - [33] G. Oya, Y. Onodera, and Y. Muto, *Low Temperature Physics-LT 13* **3**, 399 (2013).